Bold Diagrammatic Monte Carlo Technique: When the Sign Problem Is Welcome

Nikolay Prokof'ev and Boris Svistunov

Department of Physics, University of Massachusetts, Amherst, Massachusetts 01003, USA
Russian Research Center Kurchatov Institute, 123182 Moscow, Russia

(Received 23 February 2007; revised manuscript received 20 June 2007; published 18 December 2007)

We introduce a Monte Carlo scheme for sampling a bold-line diagrammatic series specifying an unknown function in terms of itself. The range of convergence of this bold(-line) diagrammatic Monte Carlo (BMC) technique is significantly broader than that of a simple iterative scheme for solving integral equations. With the BMC technique, a moderate "sign problem" turns out to be an advantage in terms of the convergence of the process. For an illustrative purpose, we solve the one-particle s-scattering problem. As an important application, we obtain the T matrix for a Fermi polaron (one spin-down particle interacting with the spin-up fermionic sea).

DOI: 10.1103/PhysRevLett.99.250201 PACS numbers: 02.70.Ss, 02.70.Tt, 05.10.Ln

The diagrammatic Monte Carlo (DMC) method [1] is a technique that allows one to simulate quantities specified in terms of convergent diagrammatic sums, i.e., sums of integrals with integrands represented by a diagrammatic structure. Formally, it is a set of generic prescriptions for organizing a systematic-error-free Metropolis-type process that samples the series or sum without explicitly taking the integrals over the internal variables in each particular term. In addition to the natural requirement of convergence, the diagrammatic sums should be either essentially finite (have only a few leading terms) or positive definite; otherwise the sign problem suppresses the efficiency of the numeric procedure. One of the key tools in the analytical diagrammatic techniques is the trick of bold lines [2] that allows one to (partially or completely) sum the series even if it is formally divergent. The bold-line trick looks also very attractive for the sign-indefinite series since it can substantially reduce the number of leading diagrams and thus alleviate the sign problem.

In this Letter, we explore the possibility of employing the bold-line trick in the DMC approach. We propose a scheme which we call the bold(-line) diagrammatic Monte Carlo (BMC) technique. In essence, the BMC technique is a generalized iterative scheme in which the iteration protocol depends on the number of iteration steps, or, equivalently, in which the next iteration is a function of not only its immediate ancestor but of the (properly weighted) whole list of earlier iterations. The crucial difference between BMC and a naïve iteration protocol—when one simply uses DMC to perform an integration for a given iteration step—is that the convergence of BMC has essentially broader parameter range. We perform an illustrative simulation for one-particle s-scattering problem. Despite its formal simplicity, the problem contains all the ingredients one can meet in a general case: the perturbative series diverges if the scattering potential is strong enough, and—in the case of a repulsive potential—the series is not positive definite. The simplifications which we have here are mainly quantitative rather than qualitative. The bold-line trick reduces the infinite perturbative series to just two terms. In the case of a strong attractive potential, two more terms appear in the right-hand side to secure the convergence. As an important application, we solve the problem of T matrix for a Fermi polaron [3].

The s-scattering problem (see, e.g., Ref. [4]) can be formulated in the form of a generic linear vector equation

$$|f\rangle = |b\rangle + \mathbf{A}|f\rangle, \tag{1}$$

where $|f\rangle$ is an unknown vector, $|b\rangle$ is a known vector, and $\mathbf{A}$ is a linear operator. Specifically, $|f\rangle \equiv f(q)$ is the zero-energy scattering wave function in the momentum representation, $|b\rangle \equiv -u(q)$, where $u(q) = U(q)/2\pi$, and $U(q)$ is the Fourier transform of the scattering potential. For simplicity, we work with a spherically symmetric potential. The Planck's constant and particle mass are set equal to unity. The operator $\mathbf{A}$ here acts as

$$\mathbf{A}f = -\frac{1}{\pi}\int_{-1}^{1} d\chi \int_{0}^{\infty} u(|\mathbf{q}-\mathbf{q}_1|) f(q_1) dq_1, \tag{2}$$

where $|\mathbf{q}-\mathbf{q}_1| \equiv \sqrt{q^2+q_1^2-2qq_1\chi}$. Rewriting (1) as

$$f = -u + \lambda \mathbf{A}u + (1+\lambda)\mathbf{A}f - \lambda \mathbf{A}^2 f, \tag{3}$$

we get a tool to control convergence of the Monte Carlo process by a proper choice of the free parameter λ (a discussion of this trick is given below). The potential we use in simulations is a flat spherical well or bump defined as $U(\mathbf{r}) = U_0$ at $r < 1$ and zero otherwise. For this potential,

$$u(q) = \frac{2U_0}{q^3}(\sin q - q\cos q). \tag{4}$$

Convergence.—Before turning to BMC, it is very instructive to analyze the convergence of a generalized iterative procedure (based on averaging of iterations) which is most close to the BMC scheme.

Expanding all the vectors in Eq. (1) in terms of the operator $\mathbf{A}$ eigenvector basis $\{|\phi_\xi\rangle\}$, we get

$$f_\xi = b_\xi + a_\xi f_\xi, \tag{5}$$

where $\mathbf{A}|\phi_\xi\rangle = a_\xi|\phi_\xi\rangle$, $|b\rangle = \sum_\xi b_\xi|\phi_\xi\rangle$, and $|f\rangle = \sum_\xi f_\xi|\phi_\xi\rangle$. The vector equation thus decouples into a set of independent equations for each ξ. From now on the label ξ can be omitted.

Let f_n be the nth generator for the $(n+1)$st iteration

$$\tilde{f}_{(n+1)} = b + af_n. \tag{6}$$

The quantity f_n is supposed to be a function of all $\tilde{f}_j$s with $j \le n$. As a characteristic example we take

$$f_n = \frac{\sum_{j=1}^n j^\alpha \tilde{f}_j}{\sum_{j=1}^n j^\alpha}, \tag{7}$$

where $\alpha > -1$ is a fixed parameter of the scheme. We can exclude $\tilde{f}$s and explicitly relate $f_{(n+1)}$ to f_n to see that for the deviation $\delta_n = f - f_n$ of the nth generator from the exact solution $f = b/(1-a)$ the following recursive relation in the large n limit takes place:

$$\delta_{(n+1)} = \delta_n + \frac{(1+\alpha)(a-1)}{n}\delta_n. \tag{8}$$

It implies the asymptotic behavior

$$\delta_n \propto e^{(1+\alpha)(a-1)\ln n} \qquad (n \to \infty). \tag{9}$$

Hence, the condition of convergence is

$$\mathrm{Re}\, a_\xi < 1. \tag{10}$$

Here we restore the subscript ξ to emphasize that condition (10) has to be satisfied for all the eigenvalues of the matrix $\mathbf{A}$. We see that the value of α does not determine the fact of convergence but does affect the asymptotic rate of convergence—the larger α is, the higher the rate. It is important that the convergence does not depend on the imaginary parts of a_ξ. Finally, negative real parts of a_ξ are desirable for convergence: the larger the absolute value of the negative real part, the better. [Note that the plain iterative method ($f_n \equiv \tilde{f}_n$) converges only when $|a_\xi| < 1$].

If condition (10) is not met, one can use an equation equivalent to (1), but with convergent iterative procedure. For the s-scattering problem, the matrix $\mathbf{A}$ is Hermitian and thus all its eigenvalues are real. In this case, rewriting Eq. (1) as

$$|f\rangle = |b\rangle + \mathbf{A}|f\rangle + \lambda\mathbf{A}(|f\rangle - |b\rangle - \mathbf{A}|f\rangle) \tag{11}$$

and fine-tuning the value of the constant λ, one can render the iterative process converging. Indeed, the new equation has the same form as the original one, up to replacements $|b\rangle \to |b\rangle - \lambda\mathbf{A}|b\rangle$ and $\mathbf{A} \to (1+\lambda)\mathbf{A} - \lambda\mathbf{A}^2$. Correspondingly, condition (10) for the new matrix will be met if the original eigenvalues satisfy the inequality

$$(1+\lambda)a_\xi - \lambda a_\xi^2 < 1. \tag{12}$$

As is easily checked, condition (12) is met provided $\lambda \in (\lambda_1, \lambda_2)$, where

$$\lambda_1^{-1} = \min_{a_\xi > 1}\{a_\xi\}, \qquad \lambda_2^{-1} = \max_{a_\xi \in (0,1)}\{a_\xi\}. \tag{13}$$

Hence, if the eigenvalues are real and separated from unity by a finite gap, there exists a value of λ at which convergence is guaranteed. Incidentally, the problem (1) can always be reformulated in such a way that the new matrix is Hermitian:

$$|f\rangle = (1 - \mathbf{A}^\dagger)|b\rangle + (\mathbf{A} + \mathbf{A}^\dagger - \mathbf{A}^\dagger\mathbf{A})|f\rangle. \tag{14}$$

Monte Carlo procedure.—Now we explain how generic DMC rules [1] can be used to calculate $f(q)$ self-consistently. For brevity, let us index the four terms in the right-hand-side of Eq. (3) as terms $\mathcal{A}$, $\mathcal{B}$, $\mathcal{C}$, and $\mathcal{D}$. Correspondingly, the "configuration space" of the problem is defined by the term index and all continuous variables associated with it. The goal of the Monte Carlo procedure is to perform stochastic summation over this configuration space. The contribution of each state to the answer is characterized by the weight with the sign, which in our case is given by the product of u and $f$functions; for example, the weight and sign of the $(\mathcal{B}, q, q', \chi)$ state are determined by the modulus and sign of $u(|\boldsymbol{q} - \boldsymbol{q}'|)f(q')$.

The standard Metropolis-type protocol consists of updates which change the current configuration state, followed by measurements which evaluate contributions of the current state to the answer. The updating scheme described below generates states with probabilities proportional to their weight. In this case, the Monte Carlo estimator for $f(q)$ is given by the state sign. The statistics of ± 1 contributions is accumulated into the $f(q)$ histogram with bins covering the positive-q axis. Apart from representing the final result of the simulation, the histogram is used self-consistently to generate random variables from the probability density $|f(q)|$ and to determine the sign of $\mathcal{B}$ and $\mathcal{D}$ states.

A straightforward accumulation of data into the histogram corresponds to $\alpha = 1$ in Eq. (7). However, large values of α result in faster convergence; see Eq. (9). Numerically, the limit of $\alpha \to \infty$ is implemented by "forgetting" old histogram data.

The simplest updating scheme contains three pairs of complementary updates $[\mathcal{A} \to \mathcal{B},\ \mathcal{B} \to \mathcal{A}]$, $[\mathcal{A} \to \mathcal{C},\ \mathcal{C} \to \mathcal{A}]$, $[\mathcal{C} \to \mathcal{D},\ \mathcal{D} \to \mathcal{C}]$ which change the term index and one self-complementary update $\mathcal{A} \leftrightarrow \mathcal{A}$ changing the variable q.

$\mathcal{A} \leftrightarrow \mathcal{A}$ *update.*—A new value for the variable q in state $\mathcal{A}$ is generating from the normalized probability density

$$p(q) = |u(q)|/I_u, \qquad I_u = \int_0^\infty |u(q)|dq. \tag{15}$$

The acceptance ratio for the $\mathcal{A} \leftrightarrow \mathcal{A}$ update is unity.

$\mathcal{A} \to \mathcal{B}$ *update.*—First, we select the value of χ from the uniform probability density on the [-1, 1] interval.

Next, we select the value q' from the histogram-based probability distribution $|f(q')|$. The acceptance ratio for this update is

$$R_{\mathcal{A}\to\mathcal{B}} = \frac{2|1+\lambda|I_f}{\pi p_{\mathcal{A}\mathcal{B}}} \left| \frac{u(\boldsymbol{q}-\boldsymbol{q}')}{u(q)} \right|, \tag{16}$$

where $p_{\mathcal{A}\mathcal{B}}$ is the probability to apply the $\mathcal{A}\to\mathcal{B}$ update while in state $\mathcal{A}$ (we do not mention the probability of applying an update to the current configuration if it is unity; in this scheme $p_{\mathcal{B}\mathcal{A}}=1$).

$$I_f = \int_0^\infty |f(q)|dq \tag{17}$$

is the normalization integral proportional to the sum of absolute values of all histogram contributions (its proper normalization is discussed below).

$\mathcal{B}\to\mathcal{A}$ update.—Here we propose to change the term index back to $\mathcal{A}$; the acceptance ratio for this move is simply the inverse of $R_{\mathcal{A}\to\mathcal{B}}$.

$\mathcal{A}\to\mathcal{C}$ and $\mathcal{C}\to\mathcal{A}$ updates.—Formally, this pair of updates is identical in implementation to the previous one, with the only difference that the value of q' in the $\mathcal{A}\to\mathcal{C}$ move is generated from the probability density $|u(q')|$. Correspondingly, the acceptance ratio is based on the I_u integral:

$$R_{\mathcal{A}\to\mathcal{C}} = \frac{1}{R_{\mathcal{C}\to\mathcal{A}}} = \frac{2|\lambda|I_u p_{\mathcal{C}\mathcal{A}}}{\pi p_{\mathcal{A}\mathcal{C}}} \left| \frac{u(\boldsymbol{q}-\boldsymbol{q}')}{u(q)} \right|. \tag{18}$$

$\mathcal{C}\to\mathcal{D}$ and $\mathcal{D}\to\mathcal{C}$ updates.—These are an exact copy of the $\mathcal{A}\to\mathcal{B}$ and $\mathcal{B}\to\mathcal{A}$ pair in terms of how new variables are proposed and removed. The acceptance ratio is

$$R_{\mathcal{C}\to\mathcal{D}} = \frac{1}{R_{\mathcal{D}\to\mathcal{C}}} = \frac{2I_f}{\pi p_{\mathcal{C}\mathcal{D}}} \left| \frac{u(\boldsymbol{q}'-\boldsymbol{q}'')}{u(q')} \right|. \tag{19}$$

The above set of updates is ergodic; i.e., it samples the entire configuration space. In the practical implementation of the algorithm we used $p_{\mathcal{A}\mathcal{A}}=0.2$, $p_{\mathcal{A}\mathcal{B}}=p_{\mathcal{A}\mathcal{C}}=0.4$, and $p_{\mathcal{C}\mathcal{A}}=p_{\mathcal{C}\mathcal{D}}=0.5$. To complete the description we have to explain how to find the normalization integral I_f. Let Z_{MC} be the total number of Monte Carlo states in the simulation and $Z_{\mathcal{A}}$ the number of $\mathcal{A}$ states. In the statistical limit,

$$\frac{Z_{\mathcal{A}}}{Z_{\mathrm{MC}}} = \frac{I_u}{I}, \tag{20}$$

I is the auxiliary "global partition function" which drops out from all final answers. If H_s is the sum of all contributions to the sth bin of the histogram, then in the statistical limit,

$$\frac{H_s}{Z_{\mathrm{MC}}} = I^{-1}\int_{q\in\mathrm{bin}_s} f(q)dq. \tag{21}$$

If we now write the normalization integral as a sum over the histogram (in the limit of infinitesimally small bin size the relation is exact),

$$I_f = \sum_s \left| \int_{q\in\mathrm{bin}_s} f_0(q)dq \right| = (Z/Z_{\mathrm{MC}})\sum_s |H_s|, \tag{22}$$

and use Eq. (20) to eliminate I/Z_{MC}, we finally arrive at

$$I_f = \frac{\sum_s |H_s|}{Z_{\mathcal{A}}} I_u. \tag{23}$$

Similarly, the scattering wave function is given by

$$f(q_s) = \frac{H_s}{Z_{\mathcal{A}}} I_u. \tag{24}$$

The s-wave scattering length can be obtained in two ways: from the $q\to 0$ limit, $a=-f(q=0)$, and as a histogram sum (the last procedure gives better accuracy since it is based on all Monte Carlo data and thus is not susceptible to the noise in a particular bin):

$$\begin{aligned} a &= u(0) + \frac{2}{\pi}\int_0^\infty u(q)f(q)dq \\ &\to u(0) + \frac{2I_u}{\pi Z_{\mathcal{A}}}\sum_s u(q_s)H_s. \end{aligned} \tag{25}$$

We have tested our BMC scheme against the analytical answer for the scattering length in different regimes which included strong repulsive and attractive potentials outside of the convergence limits for the standard iterative scheme. For example, one can easily get results for a with four-digit (or higher) accuracy for the repulsive potential $U_0=10$; a straightforward summation of the series expansion for large positive values of U_0 would be impossible because of the divergence and/or the sign problem. Series divergence will also prevent one from going across the resonance and getting results for potentials with bound states. In Fig. 1 we present data for the scattering wave function obtained for $U_0=-3$, i.e., for the potential well with the bound state. In this simulation a was obtained with the four-digit accuracy. For negative values of $U_0<-10$ we found that good initial conditions, e.g., results of the previous run for smaller $|U_0|$, are important for convergence which was very slow and required that $\lambda\approx 1$.

Fermi polaron T matrix.—The Fermi polaron is a spin-down particle interacting with the sea of spin-up fermions. Of special interest is the case when the spin-up sea is an ideal Fermi gas while the interaction between spin-up and spin-down particles is short-ranged but resonantly strong. In this regime—relevant to the notorious problem of BCS-BEC crossover in the limit of extreme population imbalance between the two fermionic components [5,6]—there is, in particular, a critical point in the interaction strength when the ground state of the polaron becomes a bound spin-zero state (molecule). The Fermi polaron problem allows an unbiased numeric solution by DMC. The relevant diagrams are constructed out of the three types of

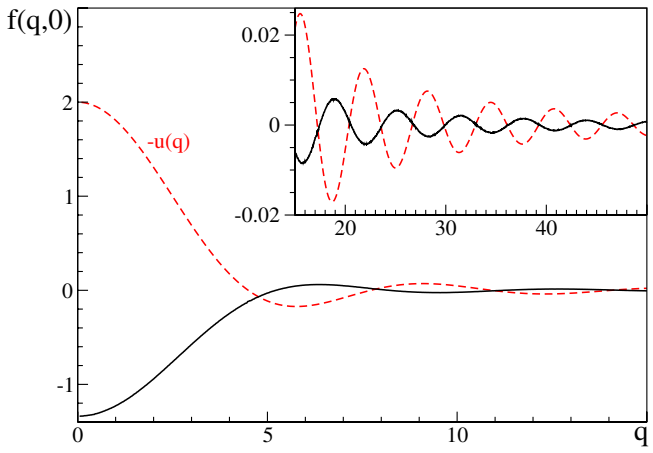

FIG. 1 (color online). Scattering wave function at zero energy (solid line) and scattering potential (dashed line) for the attractive potential well with one bound state ($U_0 = -3$).

propagators (in the imaginary-time–momentum representation): (i) spin-up Green's functions, (ii) spin-down vacuum propagators, and (iii) the T matrix of the pair interaction between spin-up and spin-down particles [3]. While simple analytic expressions for type (i) and (ii) propagators are available, the T matrix has to be tabulated numerically; this tabulation represents the performance bottleneck for the whole scheme. Noting that the equation defining the T matrix through itself (see Fig. 2) is analogous to that for the scattering amplitude, one can directly apply the above-described BMC procedure for obtaining the T matrix. We have successfully done that, which ultimately allowed us to solve the Fermi polaron problem [3].

Conclusions and outlook.—We have found a numeric counterpart to the bold-line trick of diagrammatic technique. The resulting scheme simulates unknown functions specified by diagrammatic series in terms of themselves. We illustrated our approach by solving the s-scattering problem in strong repulsive and attractive potentials. We introduced tools to secure convergence of the process. With these tools we were able to solve the s-scattering problem even in an attractive potential with a bound state—an essentially non-ground state problem.

FIG. 2. The diagrammatic equation for the T matrix (heavy dashed line) in terms of the vacuum T matrix (light dashed line), spin-down vacuum propagator (straight solid line), and truncated (to the momenta less than Fermi momentum) spin-up propagator (solid arc).

The standard many-body diagrammatic technique deals with three functions that are expressed through each other: Green's function, self-energy, and the four-point vertex. The generalization of the scheme to this case is theoretically straightforward, since one can think of them as different components of the vector $|f\rangle$. The two practical questions that are immediately seen—in the order of their importance—are: (i) convergence of the scheme and (ii) optimal data structure. The convergence of the scheme may be achieved by the tools described in this Letter, in combination with resummation techniques if necessary. If the initial approximation is close enough to the exact answer—which will be the case if one starts with an almost ideal system and moves to strong interactions by small steps in the coupling constant—then one may rely on linearization for constructing the correcting part of the right-hand side operator, similar to Eq. (11). Histograms may well be not the best method to deal with many continuous variables. Instead one may use variable-step meshes and, correspondingly, reweighing techniques for collecting statistics. Another option is to approximate unknown functions with analytic expressions and permanently optimize their parameters to best fit coarse-grained histogram sampling coming from BMC.

The work was supported by the National Science Foundation under Grant No. PHY-0426881 and Grant No. PHY-0653183.

[1] N. V. Prokof'ev, B. V. Svistunov, and I. S. Tupitsyn, JETP **87**, 310 (1998); N. V. Prokof'ev and B. V. Svistunov, Phys. Rev. Lett. **81**, 2514 (1998).

[2] Heavy (bold) lines are used for denoting exact Green's functions, light lines standing for nonperturbed Green's functions. Using bold lines while introducing appropriate constraints on the diagram structure (to prevent double counting) accounts for partial summation of diagrams. [See, e.g., A. L. Fetter and J. D. Walecka, *Quantum Theory of Many-Particle Systems* (Dover, New York, 2003).]

[3] N. V. Prokof'ev and B. V. Svistunov, arXiv:0707.4259. For physics aspects of the Fermi polaron problem see Refs. [5,6].

[4] L. D. Landau and E. M. Lifshitz, *Quantum Mechanics: Non-Relativistic Theory* (Pergamon Press, New York, 1977).

[5] A. Bulgac and M. Forbes, Phys. Rev. A **75**, 031605 (2007).

[6] C. Lobo, A. Recati, S. Giorgini, and S. Stringari, Phys. Rev. Lett. **97**, 200403 (2006).